Flow-Through System Effects on *in Vitro* Analysis of Transdermal Systems

Joseph Sclafani,[1,2] James Nightingale,[1] Puchun Liu,[1] and Tamie Kurihara-Bergstrom[1]

Received November 30, 1992; accepted April 7, 1993

The development of transdermal therapeutic systems (TTS) often involves *in vitro* evaluation of formulations and prototypes using flow-through diffusion cells. The apparent flux obtained from such methodologies does not accurately represent the actual (intrinsic) permeation of the compound through the skin. Flow-through system parameters, i.e., fraction collector tube volume, receiver cell volume, flow rate, and sampling interval, modify the flux yielding an apparent flux. Both finite-dose flux profiles and infinite-dose diffusional lag times are modified by these parameters. In this study, a transfer function is derived which describes the effect of these parameters. The intrinsic flux is calculated from apparent flux data using the transfer function and experimental flow-through system parameters. This allows the calculation of permeant flux profiles devoid of modification by the experimental methodology.

KEY WORDS: apparent flux; transfer function; intrinsic flux; flow-through system; transdermal drug delivery.

INTRODUCTION

The *in vitro* evaluation of controlled release systems such as transdermal drug delivery often involves the use of flow-through receiver systems with automated sample collection. These systems provide complete permeant release profiles and by judicious flow rate selection maintain near-sink conditions in the receiver chamber without frequent manual sampling.

Typically, the apparent flux is calculated by multiplying the permeant concentration in the fraction collector test tube by the receiver flow rate and dividing by the diffusional area. Unfortunately, the resulting delivery profile is not the intrinsic flux from the device or through the skin, since it depends on experimental flow-through system parameters.

While the effects of flow-through experimental systems commonly used to investigate transdermal release kinetics have been discussed qualitatively (1,2), the quantitative analysis of experimental parameters has received little attention. The aim of this work is to quantify these effects, extending previous mass transfer studies (3–6). A method whereby the intrinsic flux profile can be resolved from the apparent flux is also presented. The experimental flux of ethanol from a finite-dose system was used to validate this approach.

MATERIALS AND METHODS

Materials

NaCl (Mallinckrodt, Paris, KY), gentamicin sulfate (Sigma Chemical Co., St. Louis, MO), and 200 proof ethanol (USI Chemicals) were used as received. Solutions were prepared with 18-MΩ · cm purified water (Milli-Q Water System). Dermatomed human cadaver skin of transplantable quality was stored at −80°C. Intact epidermis was isolated by the method of Kligman and Christophers (7).

Permeation Experiments

Vertically assembled LGA cells (Laboratory Glass Apparatus Inc., Berkeley, CA) with a nominal diffusional area of 5 cm^2 and a measured receiver chamber volume (V_{CST}) of 6.5 mL were maintained at 32°C (Haake, Germany) and the receiver chamber contents were stirred at 600 rpm with small Teflon-coated magnetic stirrers. A Teflon tube with a volume of 0.5 mL (V_{TUBE}) was used to connect the cells to a Retriever II fraction collector (Isco, Inc., Lincoln, NB) set for hourly collection into tared test tubes. A Rabbit peristaltic pump (Rainin Instr. Co., Inc., Woburn, MA) fitted with Fisher (Pittsburgh, PA) Accu-Rated pump tubes provided continuous flow at 4.74 mL/hr (F).

Direct contact between the finite donor solution [500 μL of 50% (v/v) aqueous ethanol] and the skin was achieved using 5-cm^2 fillable transdermal therapeutic systems (FTTS) (8). The FTTS was adhered to the stratum corneum side of the epidermis and clamped on a LGA cell which had been previously filled with a degassed saline (0.15 M NaCl) receiver solution containing 0.01% (w/v) gentamicin sulfate. Ethanol concentrations in the receiver solution were assayed by gas chromatography (9).

Numerical inversion of the Laplace transforms was accomplished using Laplace from MicroMath Inc. (Salt Lake City, UT).

THEORETICAL

Mass Balance on Receiver System

The permeant mass balance on the receiver system requires that the distribution of permeant in each component of the system be understood. The receiver cell is modeled as an ideally mixed continuous stirred tank (CST) with volume V_{CST}. Qualitative studies on LGA cells carried out by Grummer *et al.* with potassium permanganate have visually demonstrated that these cells are well mixed (10). The experimental setup is diagrammed in Fig. 1. Plug flow (i.e., no longitudinal mixing or diffusion) is assumed in the tubing that connects the receiver cell to the fraction collector with volume V_{TUBE}. If appreciable nonidealities exist in either the CST or the tubing, the governing equations must be modified to account for residence time distributions. Fresh receiver solution and permeant, with flow rates F_1 and F_2, respectively, flow into the CST. The flow rate from the CST to the fraction collector is F_3. The test tube is changed at a regular time interval of ΔT. Since the permeant flow rate is much less than the flow rate of the receiver solution, it can be neglected. The total mass balance, assuming equal densities, simplifies to $F_1 = F_3 = F$.

[1] Pharmaceuticals Division, CIBA-Geigy Corporation, Ardsley, New York 10502.

[2] To whom correspondence should be addressed.

0724-8741/93/1000-1521$07.00/0

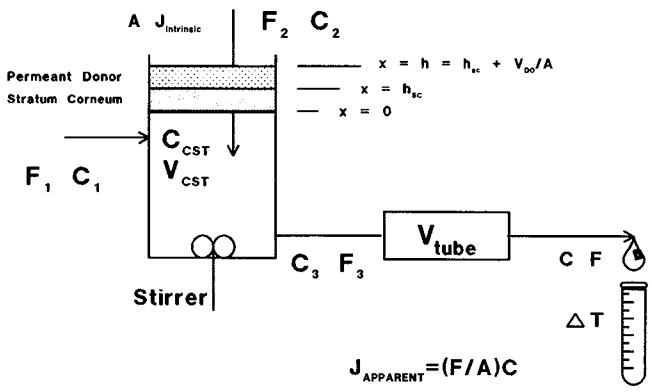

Fig. 1. Flow-through receiver system: schematic and definition of variables and parameters.

The permeant mass balance on the CST for constant CST volume is

$$V_{CST}\frac{dC_{CST}}{dt} = FC_1 + AJ_{intrinsic} - FC_3 \quad (1)$$

where C_1 is the permeant concentration in the incoming receiver solution and C_3 is the permeant concentration exiting the CST. In this balance, the net flow of permeant through the skin, F_2C_2, has been replaced with the product $AJ_{intrinsic}$, where $J_{intrinsic}$ and A denote the intrinsic mass flux of the permeant through the skin and the diffusional area, respectively. Noting that $C_1 = 0$ and that, since the CST is perfectly mixed, $C_3 = C_{CST}$, the balance becomes

$$V_{CST}\frac{dC_{CST}}{dt} = AJ_{intrinsic} - FC_{CST} \quad (2)$$

In the tubing, the concentration is not modified by mixing. However, a finite time period is required for the fluid to flow through the tube. Using the time axis shift theorem, the concentration at the tube outlet, $C(t)$, is the concentration leaving the CST after a time delay of τ_{TUBE}:

$$C(t) = \begin{cases} 0, & t < \tau_{TUBE} \\ C_{CST}(t - \tau_{TUBE}), & t \geq \tau_{TUBE} \end{cases} \quad (3)$$

where $\tau_{TUBE} = V_{TUBE}/F$, which is the residence time of the permeant in the fraction collector tubing. The apparent flux is calculated from this concentration by multiplying by the flow rate and dividing by the diffusional area. The diffusional area has a direct impact on C_{CST}. However, since the apparent flux is calculated by normalizing the C_{CST} by A, $J_{apparent}$ is independent of the diffusional area.

Combining Eqs. (2) and (3) and multiplying all terms by F/A, the linear first-order differential equation becomes

$$\tau_{CST}\frac{dJ_{apparent}(t)}{dt} + J_{apparent}(t) = J_{intrinsic}(t - \tau_{TUBE}) \quad (4)$$

where $\tau_{CST} = V_{CST}/F$ is the residence time of the permeant in the receiver cell. The initial condition for this equation is

$$J_{apparent}(0 \leq t \leq \tau_{TUBE}) = 0 \quad (5)$$

The Laplace transform of Eq. (4), subject to Eq. (5), yields the transfer function, $G(s)$:

$$G(s) = \frac{e^{-s\tau_{TUBE}}}{s\tau_{CST} + 1} \quad (6)$$

This function relates the intrinsic and apparent fluxes in Laplace space:

$$J_{apparent}(s) = G(s)J_{intrinsic}(s) \quad (7)$$

In addition to the effects of the flow-through experimental apparatus, the flux profile is also changed by the sampling interval over which the receiver solution is collected in each test tube, ΔT. Rather than representing the instantaneous concentration exiting the tube, the concentration in each test tube is the average exiting concentration during this sampling period. The calculation of the experimental apparent flux at time t must be amended to reflect this finite sampling interval. Therefore, for $t \geq \Delta T$, the apparent flux is given by

$$J_{apparent}^{experimental}\left(t - \frac{\Delta T}{2}\right) = \frac{F}{A}\frac{1}{\Delta T}\left[\int_{t-\Delta T}^{t} C(\theta)d\theta\right] = \frac{F}{A}\bar{C}\left(t - \frac{\Delta T}{2}\right) \quad (8)$$

where the bar over the concentration, C, represents the average concentration over ΔT at the average time $t - \Delta T/2$.

Intrinsic Flux from Apparent Flux Data

In transdermal drug delivery, it is important to determine the rate at which the permeant crosses the skin and enters the systemic circulation. The aim of this part of the study is to use the transfer function derived above to calculate this intrinsic flux of the permeant from an experimentally determined apparent flux profile. The apparent flux profile is fitted to an appropriate curve:

$$J_{apparent}^{experimental}(t) = a[e^{-bt} - e^{-ct}] \quad (9)$$

This equation has been found to describe the experimental data well. It is derived from an assumed exponential decaying donor concentration for a permeant with a short diffusional lag time through the stratum corneum (intrinsic lag time). The parameters a, b, and c have physical significance and are determined by the method of least squares. Taking the Laplace transform of Eq. (9) yields

$$J_{apparent}^{experimental}(s) = \left[\frac{a}{(s+b)} - \frac{a}{(s+c)}\right] \quad (10)$$

According to Eq. (7), this expression, divided by the transfer function, $G(s)$, gives the intrinsic flux in Laplace space. The resulting expression can then be inverted to yield the dependence of intrinsic flux on time:

$$J_{intrinsic}(t) = L^{-1}\left[\frac{J_{apparent}(s)}{G(s)}\right] \quad (11)$$

This yields an experimental intrinsic flux profile without modification by the *in vitro* receiver system.

RESULTS AND DISCUSSION

Using Fick's second law, a theoretical intrinsic flux pro-

file was calculated for representative skin and donor parameters appropriate for percutaneous ethanol delivery. The diffusion equations and their corresponding initial and boundary conditions are summarized in Table I. Convection in the donor chamber is several orders of magnitude smaller than diffusion for this study, since the velocity in the donor chamber is determined by the permeant diffusivity in the skin. This justifies the use of Fick's law. The intrinsic flux profiles are represented in Figs. 2, 3, and 4 as solid lines. From this profile, apparent flux profiles (dashed lines) were calculated as a function of experimental system parameters. It has been shown that D_{SC} and K change with ethanol concentration (11). Although there is an ethanol gradient across the stratum corneum and a corresponding gradient in D_{SC} and K, approximate constant values are used here since the goal was to examine the effect of the experimental system on the measured flux. The D_{SC} was approximated from the permeability coefficient (12):

$$P = \frac{D_{SC}}{h_{SC}} K \tag{12}$$

where P and h_{SC} are 10^{-6} cm/sec (11) and 20 μm (12), respectively, and K (13,14) is as listed with the figures. The diffusivity in the donor chamber, D_{DO}, was obtained from the literature (15).

Effect of Flow-Through System Parameters on Apparent Flux

Experimentally, V_{TUBE}, V_{CST}, F, and ΔT can be varied; their effects on the apparent flux are depicted in Figs. 2, 3, 4, and 5, respectively. The shape of the intrinsic flux profile reaches a peak rapidly and then decays as the donor is depleted. This is dramatically different than the apparent flux profiles which are calculated using common system parameters.

The impact of V_{TUBE} on the apparent flux profile is shown in Fig. 2, where the flow rate is constant and τ_{TUBE} is varied by changing the tube volume, V_{TUBE}. Note that

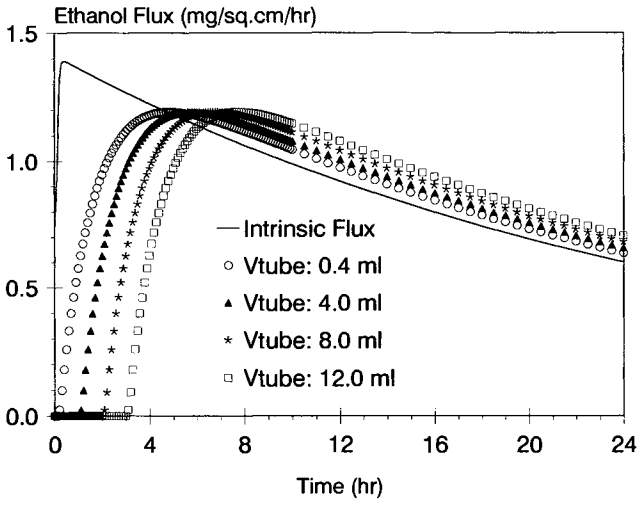

Fig. 2. Effect of V_{TUBE} on apparent flux. F = 4 mL/hr, V_{CST} = 6 mL (τ_{CST} = 1.5 hr), and ΔT = 0. K = 1, h_{SC} = 20 μm, D_{SC} = 2×10^{-9} cm²/sec, V_{DO} = 0.5 mL, D_{DO} = 10^{-5} cm²/sec, C^0_{DO} = 395 mg/mL, and A = 5 cm².

τ_{TUBE} affects only a time delay of the permeant. If V_{TUBE} is reduced, the time delay will also be decreased for a constant flow rate. The residence time in the tubing should be subtracted from the experimental time to account for this delay.

Figure 3 illustrates the effect of varying V_{CST} (τ_{CST}) on the apparent flux for which τ_{TUBE} and F are held constant. Barry has discussed the importance of receiver solution turnover in flow-through cells as it relates to maintaining sink conditions (16). There is a delay as well as a reduction in permeant concentration as it flows through the cell, as demonstrated by longer times to peak flux and lower peak height. V_{CST} should be minimized to reduce these effects. While the residence time in the cell may be subtracted from the experimental time to account for the delay, the dilution effect can be accounted for as described under Intrinsic Flux Calculation From Apparent Data.

Table I. Theoretical Intrinsic Flux Profile

Diffusion equations	Initial conditions	Boundary conditions[a]
$\frac{\partial C_{DO}}{\partial t} = D_{DO}\frac{\partial^2 C_{DO}}{\partial x^2}$ $h > x > h_{SC}$	$C_{DO} = C^0_{DO}$	$\left.\frac{\partial C_{DO}}{\partial x}\right\|_{x=h} = 0$
		$D_{DO}\left(\frac{\partial C_{DO}}{\partial x}\right)\Big\|_{x=h_{SC}} = D_{SC}\left(\frac{\partial C_{SC}}{\partial x}\right)\Big\|_{x=h_{SC}}$
		$K = \left.\frac{C_{SC}}{C_{DO}}\right\|_{x=h_{SC}}$
$\frac{\partial C_{SC}}{\partial t} = D_{SC}\frac{\partial^2 C_{SC}}{\partial x^2}$ $h_{SC} > x > 0$	$C_{SC} = 0$	$D_{SC}\left(\frac{\partial C_{SC}}{\partial x}\right)\Big\|_{x=0} = J_{intrinsic}$

[a] See Fig. 1 for a schematic representation of the coordinate system.

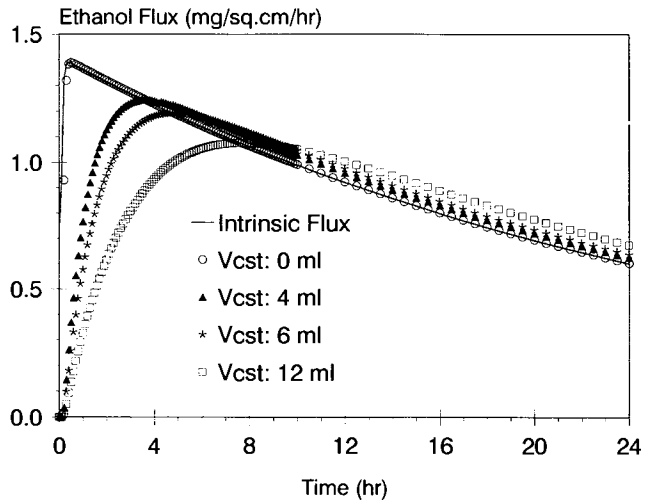

Fig. 3. Effect of V_{CST} on apparent flux. F = 4 mL/hr, V_{TUBE} = 0.4 mL (τ_{TUBE} = 0.1 hr), and ΔT = 0. K = 1, h_{SC} = 20 μm, D_{SC} = 2 × 10^{-9} cm^2/sec, V_{DO} = 0.5 mL, D_{DO} = 10^{-5} cm^2/sec, C^0_{DO} = 395 mg/mL, and A = 5 cm^2.

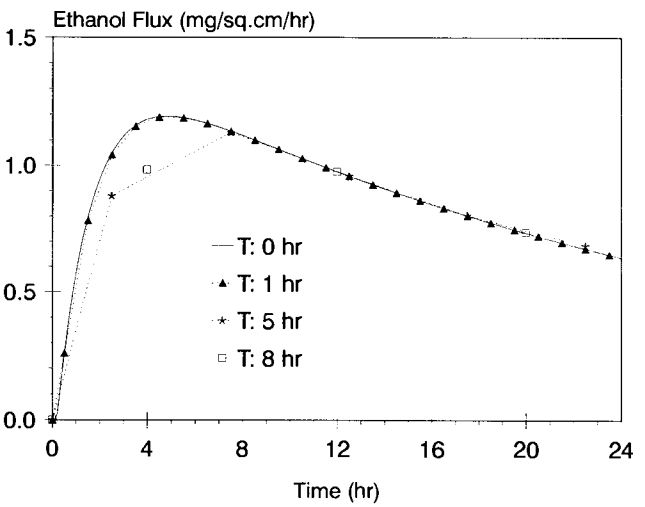

Fig. 5. Effect of the sampling interval on apparent flux. F = 4 mL/hr, V_{TUBE} = 0.4 mL (τ_{TUBE} = 0.1 hr), and V_{CST} = 6 mL (τ_{CST} = 1.5 hr). K = 1, h_{SC} = 20 μm, D_{SC} = 2 × 10^{-9} cm^2/sec, V_{DO} = 0.5 mL, D_{DO} = 10^{-5} cm^2/sec, C^0_{DO} = 395 mg/mL, and A = 5 cm^2.

Experimentally, F can be varied while holding the cell and tube volumes constant for a given receiver system. In Fig. 4, it is evident that the modification of the apparent flux is a strong function of the flow rate, which should be maximized. This is supported by the findings of Crutcher and Maibach (17). There are several practical constraints on the flow rate, however. For example, too fast a flow rate may lead to test tube concentrations which lie below the limits of detection. Alternatively, if the flow rate is too slow, exceeding sink conditions may become a problem. Also, high flow rates may lead to high pressures in V_{CST} and excessive skin deformation.

The apparent flux profiles discussed above are instantaneous profiles, that is, the fraction collector interval, ΔT, approaches zero. Experimentally, the permeant is collected over a finite, nonzero sampling interval. As ΔT is increased, information is lost during the concentration averaging which takes place in the fraction collector test tube. To illustrate this point, τ_{CST}, τ_{TUBE}, and F were held constant and ΔT was varied. The average flux values were plotted vs the average time, that is, at $t - \Delta T/2$. As shown in Fig. 5, the longer sampling interval both decreases the peak height and skews the peak to longer times. For these residence times, the one hour interval overlaps the instantaneous curve. This is due to the concentration averaging which had previously occurred in the CST (τ_{CST} = 1.5 hr). When the interval is increased to 5 or 8 hr, the deviation in the profile is evident. The optimal sampling interval is a compromise between resolution and the number of samples which must be handled per experiment. For example, halving the sampling interval and analyzing every other test tube will increase accuracy without doubling the necessary work load.

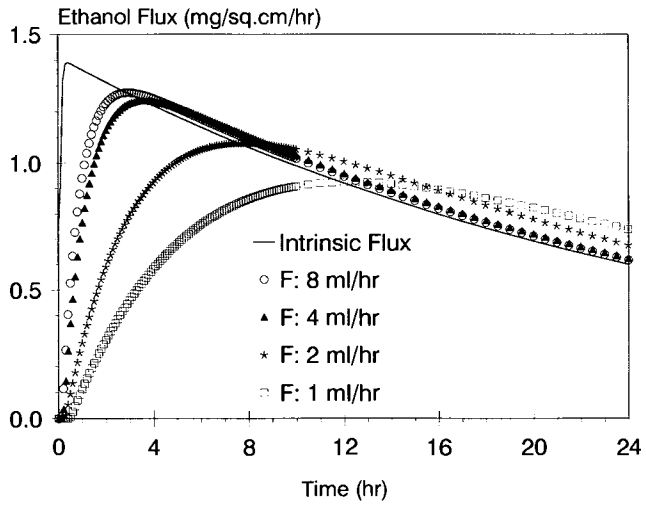

Fig. 4. Effect of flow rate on apparent flux. V_{TUBE} = 0.4 mL, V_{CST} = 6 mL, and ΔT = 0. K = 1, h_{SC} = 20 μm, D_{SC} = 2 × 10^{-9} cm^2/sec, V_{DO} = 0.5 mL, D_{DO} = 10^{-5} cm^2/sec, C^0_{DO} = 395 mg/mL, and A = 5 cm^2.

The diffusional areas and volumes differ widely among commercially available diffusion cells, as shown in Table II. The additional parameters, V_{TUBE}, F, and ΔT, can be optimized by the experimenter within limits through the judicious selection of tubing, receiver flow rate, and fraction collector interval.

Intrinsic Flux Profile Calculation from Apparent Data

The transfer function can also be used to calculate an

Table II. Several Commercially Available Flow-Through Cells

	Area (cm^2)[a]	V_{CST}(mL)
Crown Glass Co.		
Side by side	0.695	3.4
Flow-through Franz	0.2 → 5	11.5
Laboratory Glass Apparatus Inc.		
1084-SPC	1.0	3.2
1084-MPC	3.3	5.9
1084-LPC	5.0	6.5

[a] Nominal value.

intrinsic flux from experimental apparent flux data. These flux data are shown in Fig. 6 for ethanol permeation. In this case, the sampling interval was every hour, but only selected samples were analyzed. Flux values are reported at the average time over the sampling interval, as in Eq. (8). The experimental apparent flux profile was fitted to Eq. (9), although any equation which represents the data well may be used. Using Eq. (11), which incorporates the actual system parameters for this experiment, the intrinsic flux was calculated.

The resulting intrinsic flux profile is very similar to the theoretical curves calculated above. There is a slight deviation from the theoretical profile at short times which may be due to several sources. First, the experimental apparent flux is an average flux due to mixing in the CST over τ_{CST} as well as in the fraction collector test tube over the collection interval ΔT. There is an irreversible loss of information on taking these averages. This is most pronounced at short times, because the concentration is changing rapidly. Second, as shown above, the modification of the apparent flux for a given experimental setup is strongly dependent on the flow rate. Error in the measured flow rate decreases the accuracy of this calculation.

Retrieval of the intrinsic flux using numerical inversion of Eq. (11) need not be carried out for each experiment. As long as F, V_{CST}, V_{TUBE}, and ΔT are known, data manipulation can be performed at a later date. The intrinsic flux is desired when comparing data obtained from non-flow-through systems or flow-through systems which use different flow-through parameters. This manipulation is easily performed on a personal computer.

Infinite Donor Effects

The unsteady portion of a flux profile from an infinite donor is also affected by the receiver system. This is illustrated in Fig. 7, where cumulative curves are plotted for the apparent as well as intrinsic data. Typically, the lag time is determined by the x intercept of the regression line for the steady-state portion of the plot (18). This figure illustrates the difference between the intrinsic and apparent lag times. The intrinsic diffusional lag time of the permeant through the skin is obtained from the intrinsic flux. The apparent lag time from Fig. 7 is the sum of the intrinsic lag time and the residence times in the CST and tubing. Therefore, the intrinsic lag time can be obtained from experimental data by subtracting both τ_{CST} and τ_{TUBE} from the apparent lag time.

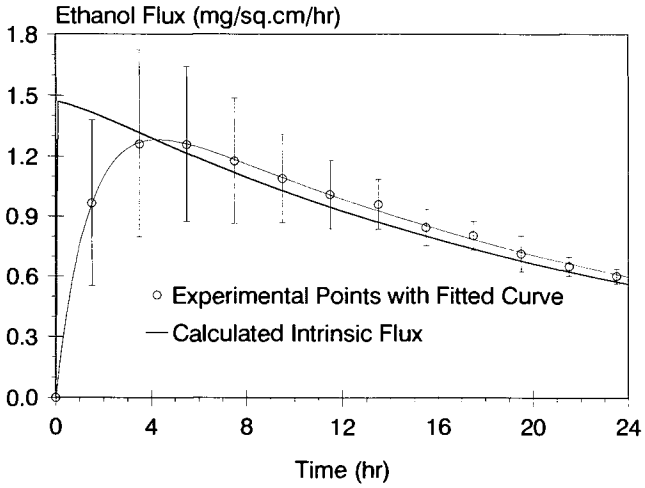

Fig. 6. Calculated intrinsic flux determined from experimental apparent flux data using the transfer function. F = 4.74 mL/hr, V_{CST} = 6.5 mL, V_{TUBE} = 0.5 mL, and A = 5 cm^2. Experimentally, the 50% aqueous ethanol donor, with V_{DO} of 0.5 mL, was run with ΔT equal to 1 hr. The error bars are standard deviation for 12 replicates.

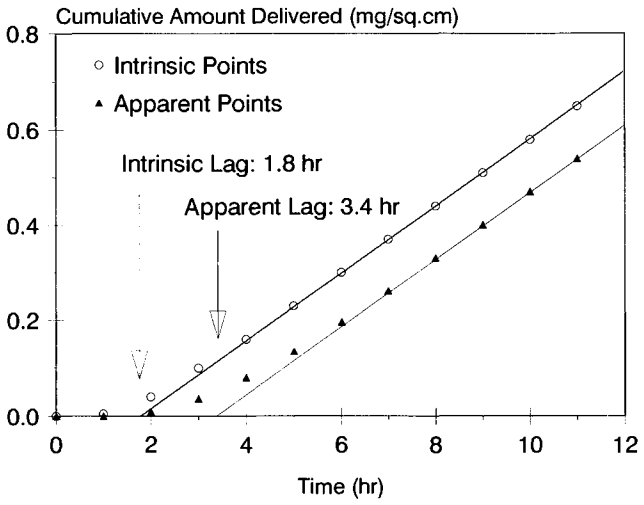

Fig. 7. Effect of flow-through parameters on lag times estimated from infinite donors. K = 1, h_{SC} = 20 μm, D_{SC} = 10^{-10} cm^2/sec, V_{DO} = 25 mL, D_{DO} = 10^{-5} cm^2/sec, C^0_{DO} = 395 mg/mL, and A = 5 cm^2. The flow-through parameters are F = 4 mL/hr, V_{TUBE} = 0.4 mL (τ_{TUBE} = 0.1 hr), V_{CST} = 6 mL (τ_{CST} = 1.5 hr), and ΔT = 0.

CONCLUSION

Commonly used flow-through systems used to examine skin penetration, from both finite and infinite donor solutions, modify the flux profiles and lag times yielding apparent results. In the optimization of finite donor systems, it is important to know the intrinsic TTS delivery. We have demonstrated that, relative to the intrinsic flux, the apparent flux profile from a finite donor is delayed and that the maximum flux is reduced due to typical experimental setups. Also, the lag time calculated from infinite donor apparent flux data includes delays due to permeant residence times in the diffusion cell and fraction collector tube. Investigators should take this delay into account when reporting data. To minimize the flow-through system effects, the flow rate should be maximized and the fraction collector interval minimized. The volumes of both the receiver cell and the tubing leading from the receiver cell to the fraction collector should also be minimized. The average apparent flux from test tube concentration data should be reported at the average time over which it was collected, not at the end of the collection interval. Finally, a transfer function has been presented for calculating the actual flux through the skin, that is, intrinsic flux from experimental apparent flux data.

ACKNOWLEDGMENTS

The authors wish to express their appreciation to Dr. K.

Stebe, Dr. C. Maldarelli, and Mr. B. Kapoor for their valuable insight and suggestions and to Mr. C. Mirley for performing the *in vitro* flux experiments.

REFERENCES

1. R. L. Bronaugh and R. F. Stewart. Methods for in vitro percutaneous absorption studies. IV. The flow-through diffusion cell. *J. Pharm Sci.* 74:65–67 (1985).
2. R. L. Bronaugh. A flow-through diffusion cell. In R. L. Bronaugh and H. I. Maibach (eds.), *In Vitro Percutaneous Absorption: Principles, Fundamentals, and Applications,* CRC Press, Boston, 1991, pp. 17–23.
3. R. H. Guy and J. Hadgraft. A theoretical description relating skin penetration to the thickness of the applied medicament. *Int. J. Pharm.* 6:321–332 (1980).
4. W. J. Addicks, G. Flynn, N. Weiner, and R. Curl. A mathematical model to describe drug release from thin topical applications. *Int. J. Pharm.* 56:234–248 (1989).
5. W. Addicks, N. Weiner, G. Flynn, R. Curl, and E. Topp. Topical drug delivery from thin applications: Theoretical predictions and experimental results. *Pharm. Res.* 7:1048–1054 (1990).
6. P. P. Bhatt, M. S. Hanna, P. Szeptycki, and T. Higuchi. Finite dose transport of drugs in liquid formulations through stratum corneum: Analytical solution to a diffusion model. *Int. J. Pharm.* 50:197–203 (1989).
7. A. M. Kligman and E. Christophers. Preparation of isolated sheets of human stratum corneum. *Arch. Dermatol.* 88:702–705 (1963).
8. J. Nightingale, F. Hischak, and T. Kurihara-Bergstrom. A fillable transdermal therapeutic system (FTTS) for *in vitro* and clinical evaluations. *Pharm. Res.* 7:s-194 (1990).
9. T. Kurihara-Bergstrom, L. DeNoble, and C. Goates. Percutaneous absorption enhancement of an ionic molecule by ethanol-water systems in human skin. *Pharm. Res.* 7:762–766 (1990).
10. C. Grummer, R. Hinz, and H. I. Maibach. The skin penetration cell: a design update. *Int. J. Pharm.* 40:101–104 (1987).
11. P. Liu, T. Kurihara-Bergstrom, and W. R. Good. Cotransport of estradiol and ethanol through human skin *in vitro:* Understanding the permeant/enhancer flux relationship. *Pharm. Res.* 8:938–944 (1991).
12. W. I. Higuchi, J. L. Fox, K. Knutson, B. D. Anderson, and G. L. Flynn. The dermal barrier to local and systemic drug delivery. In R. T. Borchardt, A. J. Repta, and V. J. Stella (eds.), *Directed Drug Delivery,* HUMANA Press, NJ, 1985, pp. 97–117.
13. R. J. Scheuplein and I. H. Blank. Permeability of the skin. *Physiol. Rev.* 51:702–737 (1971).
14. R. J. Scheuplein. Percutaneous absorption: Theoretical aspects. In P. Mauvais-Jarvis, C. F. H. Vickers, and J. Wepierre (eds.), *Percutaneous Absorption of Steroids,* Academic Press, New York, 1980, pp. 1–17.
15. R. B. Bird, W. E. Stewart, and E. N. Lightfoot, *Transport Phenomena,* John Wiley & Sons, New York 1960.
16. B. W. Barry. Methods for studying percutaneous absorption. In J. Swarbrick (ed.), *Dermatological Formulations: Percutaneous Absorption,* Marcel Dekker, New York, 1983, p. 247.
17. W. Crutcher and H. I. Maibach. The effect of perfusion rate on *in vitro* percutaneous penetration. *J. Invest. Dermatol.* 53:264–269 (1969).
18. J. Crank. *The Mathematics of Diffusion,* Clarendon Press, Oxford, 1975.